

## ***Ab Initio* Studies on Organophosphorus Compounds. 6.<sup>1–5</sup> Interactions of Dimethylphosphinic and Dimethylphosphinothioic Acid Monoanions and Methylenebisphosphonic Acid Dianion with Calcium**

Jari P. Räsänen,<sup>†</sup> Esko Pohjala,<sup>‡</sup> Hannu Nikander,<sup>§</sup> and Tapani A. Pakkanen<sup>\*,†</sup>

Department of Chemistry, University of Joensuu, P.O. Box 111, FIN-80101, Joensuu, Finland, Leiras Oy, P.O. Box 33, FIN-33721, Tampere, Finland, and Leiras Oy, P.O. Box 415, FIN-20101, Turku, Finland

Received: April 9, 1997<sup>⊗</sup>

Bisphosphonates are analogues of pyrophosphate species. Two phosphonic acid groups are bonded to the carbon atom, forming the P–C–P backbone of the bisphosphonate. Several types of bisphosphonates have been developed during the past two decades. Bisphosphonates have clinical use in diagnostic and therapeutic applications in the treatment of various bone diseases and calcium metabolism. In our *ab initio* molecular orbital studies, one to three water molecules, dimethylphosphinic acid monoanions, dimethylphosphinothioic acid monoanions, and dianionic methylenebisphosphonates were bonded to the surface calcium of molecular modeled hydroxyapatite (HAP) crystal. To study additional bisphosphonate–calcium bonding, a model of the bisphosphonate–calcium–bisphosphonate complex was investigated in different conformations. All the molecular structures studied were fully optimized by a 3-21G(\*) basis set, and the molecular energies obtained were studied by means of model reactions.

### **Introduction**

A balance of calcium in the human body is very important for health. Bone resorption, osteolytic bone metastases due to breast carcinoma, multiple myeloma, Paget's bone disease, osteoporosis, bone tumors and bone cancer, hypercalciuria and hypercalcemia due to malignancy are all diseases that are strongly related to the amount and behavior of calcium in the body. Bisphosphonate analogues, e.g. clodronate ((dichloromethylene)bisphosphonic acid), are effective in the treatment of these diseases.<sup>6–10</sup> Commercially available compounds such as etidronate, clodronate, and pamidronate have successfully been used in the treatment of tumor-induced bone diseases. These three bisphosphonates effectively inhibit bone resorption, reduce pain remarkably, and have the ability to cure hypercalcemia and hypercalciuria. At the same time, treatments with bisphosphonates reduce the possibility of bone fractures and further formation of osteolytic lesions.<sup>7–14</sup>

Many pharmacological studies have been made of the various bisphosphonates, and their medicinal character has been proven through clinical observations.<sup>7,10,11–14</sup> The precise mechanism controlling the function of the bisphosphonates during the therapy is unclear.<sup>6</sup> For example, it has been postulated that clodronate molecules can act directly on the metabolism of osteoclasts, and the absence of dicationic metal ions is essential for this action.<sup>6–8,10</sup> Clodronate is thought to be fixed to the bone surface calcium until the osteoclast cells accumulate the resorbed bone remnants with the clodronate.<sup>6</sup> Once within the osteoclasts, intracellular Fe<sup>3+</sup> may be reduced to Fe<sup>2+</sup>, which replaces the Ca<sup>2+</sup> ions in the bisphosphonate–calcium complexes and causes precipitation of the bisphosphonate–iron species. Metabolic pathways dependent on intracellular iron then become unbalanced, leading to the injury or death of the osteoclast cells.<sup>6</sup>

Theoretical *ab initio* molecular orbital (MO) studies are a useful way for obtaining geometric and energetic information

for bisphosphonate–metal ion interactions. In previous studies, we have calculated the molecular geometries of methylphosphonate and methylphosphinate and their nitrogen and sulfur analogues,<sup>1</sup> methyl methylphosphonate and methyl methylphosphinate and their sulfur analogues,<sup>2</sup> and methylenebisphosphonate and (dichloromethylene)bisphosphonate structures<sup>4,5</sup> and their bonding to water molecules<sup>4</sup> and to magnesium and calcium ions.<sup>3,5</sup>

Extensive studies have been reported earlier for many biologically interesting phosphorus compounds by experimental and theoretical methods.<sup>8,9,15–28</sup>

Calcium hydroxyapatite (Ca<sub>10</sub>(OH)<sub>2</sub>(PO<sub>4</sub>)<sub>6</sub> or HAP) is the most commonly occurring calcium phosphate species and the most abundant mineral in bones and teeth and therefore suitable as the prototype for bone matrix.<sup>6,29–34</sup> Absorption of polypeptides in the HAP surface has been studied by magnetic resonance methods.<sup>35</sup> Osteocalcin-hydroxyapatite interactions in the extracellular organic bone matrix have been studied using various experimental methods.<sup>36,37</sup> Different polymorphs of divalent metal bisphosphates have been modeled by atomistic simulation techniques.<sup>24</sup> X-ray standing waves have been applied to locating calcium in membranes.<sup>38</sup> Hydroxyapatite is the prototype for inorganic material in bone<sup>29</sup> and therefore was chosen for the modeling of bone surface in our studies. It is well-known that some bisphosphonates, e.g. clodronate, are tightly bonded to the skeletal sites of bone matrix,<sup>6,13</sup> and because of this we have modeled and studied the bonding of bisphosphonates on the (001) surface of HAP crystal by *ab initio* MO methods.

### **Computational Methods**

*Ab initio* Hartree–Fock SCF-MO calculations on calcium–bisphosphonate, HAP–bisphosphonate, and HAP–water complexes were performed with Gaussian 90 and 92 programs<sup>39</sup> on SGI 4D/35, Indigo R4000/Elan, and IBM RS6000 computers. Molecular geometries were optimized in the gas phase with the 3-21G(\*) basis set. Calculated molecular structures at the 3-21G(\*) basis set level correlate well with experimental and theoretical reference results.<sup>1–4,40–48</sup> Correlation corrections

<sup>†</sup> University of Joensuu.

<sup>‡</sup> Leiras Oy, Tampere.

<sup>§</sup> Leiras Oy, Turku.

<sup>⊗</sup> Abstract published in *Advance ACS Abstracts*, June 15, 1997.

were calculated with the MP2/3-21G(\*)//3-21G(\*) method.<sup>39</sup> The basis set superposition error (BSSE) was calculated for the selected interaction systems. The neutron diffraction parameters for the hydroxyapatite crystal ( $\text{Ca}_5(\text{PO}_4)_3\text{OH}$  or HAP) evaluated by Sanger and Kuhs<sup>29</sup> were used as a model geometry for the hydroxyapatite crystal modeling. Hydrogens were added to the phosphorus groups of the HAP model to stabilize the charge effects at the edges of the model. The molecular geometry of the HAP crystal model was frozen in the original crystal structure. The  $xy$ -plane (001) of the HAP crystal was chosen to model the surface.

A self-consistent reaction field (SCRf) model, based on the code of Rivail<sup>49,50</sup> et al. and Rinaldi<sup>51,52</sup> et al., implemented in Gaussian 90 was used to produce water medium effects ( $\epsilon = 78.54^{53}$ ).<sup>39,54</sup> A single-center multipole expansion up to  $l = 6$  was used to describe the charge distribution of the solute in the SCRf model. Ellipsoidal cavities around molecules were determined by the van der Waals surfaces. The ellipsoidal cavities in the SCRf calculations and the changes in the dimensions of these cavities have been discussed earlier by Tomasi and Persico.<sup>55</sup> In our study, the dimensions of the cavities were increased by 0.5  to ensure convergence in the multipole expansions in the SCRf calculations.<sup>5</sup> The SCRf calculations were made for the frozen optimized molecular geometries calculated at the 3-21G(\*) basis set level. Mulliken charges were determined for all atoms in the structures.<sup>39</sup> The molecular modeling program Sybyl was used for drawing the molecules.<sup>56</sup>

## Results and Discussion

**Hydroxyapatite Crystal Surface Modeling.** The hydroxyapatite crystal structure was modeled by the Sybyl<sup>56</sup> molecular modeling program according to the crystal parameters, fractional coordinates, and space group evaluated by Sanger and Kuhs. The nine-coordinated calcium with the six neighboring phosphorus groups was cut away from the modeled crystal piece of hydroxyapatite in a direction perpendicular to the  $xy$ -plane of the crystal face (001). The surface calcium was made available for bonding by removing three phosphorus groups from the chosen  $xy$ -plane (001); the three other phosphorus groups below the calcium retained their original positions. Three calcium coordination sites above the surface were then available for the approaching ligands. In the crystal model, two oxygens in each remaining phosphorus groups were bonded to the surface calcium and these P···O bond lengths were 245.7 and 281.4 pm.

The original crystal structure of the model was kept geometrically unchanged in the *ab initio* MO calculations. The edges of the model were stabilized by adding hydrogens. Each of the  $\text{PO}_4^{3-}$  groups had three hydrogens in which the bonding parameters were fully optimized. As a result, the HAP crystal was presented in the form of a modeled  $[\text{Ca}(\text{H}_3\text{PO}_4)_3]^{2+}$  complex. The Mulliken charge of the calcium was 0.96 $e$  in this model. One to three water molecules, dimethylphosphinic acid or dimethylphosphinothioic acid monoanions, or a methylenebisphosphonic acid dianion was added as a ligand to the  $[\text{Ca}(\text{H}_3\text{PO}_4)_3]^{2+}$  complex.

**Water Molecules on the Hydroxyapatite Surface.** In the HAP crystal model, there are free coordination sites above the calcium cation. The normal line to the  $xy$ -plane through the surface calcium guided the approach of the first water molecule. The geometry of the water was then relaxed. In the optimized HAP–water complex **a1**, the Ca···O line was deflected 41° from the direction of the normal line to the  $xy$ -plane through the calcium. Simultaneously, a hydrogen bond was formed from

the hydrogen of the water molecule to the oxygen of the surface. The preferred Ca···O distance of 227.1 pm was calculated in the **a1** structure, and the hydrogen bond length was 195.4 pm (Figure 1 and Table 1). The hydrogen bond O–H···O angle was 128°. In the bound water molecule the H–O–H angle was 112.2°. The Mulliken charge of the calcium was 0.81 $e$ .

The bonding of two water molecules to the HAP model was studied next. The preferred Ca···O distances of 228.9 and 230.4 pm were evaluated for the optimized **a2** conformation (Figure 1 and Table 1). The Ca···O bonding directions were then deflected 46° and 55° from the normal line of the  $xy$ -plane. The calcium-bonded water molecules were also hydrogen-bonded to the oxygens of the crystal model. These hydrogen bond lengths were 188.7 and 205.1 pm. The respective O–H···O hydrogen bond angles were 124° and 128°. The H–O–H angles of the bound water molecules were 112.4° and 113.1°. The Mulliken charge of the calcium decreased to the value of 0.66 $e$  as compared to the relative value of 0.81 $e$  in the **a1** structure.

The bonding of three water molecules to the HAP surface was calculated. The distances and geometries of the water molecules were optimized. Ca···O distances ranging from 232.0 to 233.5 pm were calculated for **a3** (Figure 1 and Table 1). The Ca···O bonding directions were deflected 55°, 57°, and 58° from the normal line of the  $xy$ -plane through the surface calcium. As a comparison, *ab initio* calculations have predicted M–O distances of 239.9 pm for the hexahydrated  $[\text{Ca}(\text{H}_2\text{O})_6]^{2+}$  species, and the corresponding experimentally evaluated M–O values have ranged from 240 to 249 pm.<sup>57</sup> The interactions calculated for the water–calcium bonding on the HAP surface were supported by hydrogen bonds, and therefore the Ca···O distances are shorter than the theoretical and experimental values of the free  $[\text{Ca}(\text{H}_2\text{O})_6]^{2+}$  species. All three water molecules in the **a3** complex were also bonded to the oxygens of the HAP surface with hydrogen bond lengths of 183.9, 190.2, and 192.6 pm. The O–H···O hydrogen bond angles ranged from 128° to 133° (Table 1). In the bound water molecules, the H–O–H angles were 112.7°, 113.0°, and 113.2°. All hydrogen bonds were conventional, no double-donor–double-acceptor hydrogen bond interactions were found. Strong Ca···O interactions, with supporting hydrogen bonds from the water molecules to the surface, confirmed that water molecules stay close to the metal ion. *Ab initio* calculations at the DZP SCF level have been used to determine conventional hydrogen bond lengths in the range 176.8–197.4 pm for the local stationary points of the  $\text{PO}_3^-(\text{H}_2\text{O})_n$  complexes ( $n = 1-3$ ).<sup>41</sup> The 6-31G\* basis set calculations for  $\text{CH}_3\text{SCH}_2\text{CO}_2^-$  species with water molecules have suggested conventional hydrogen bond lengths from 181.9 to 251.3 pm.<sup>58</sup> The Mulliken charge of the calcium in the HAP model **a3** was decreased to the value of 0.52 $e$ . The difference was 0.29 $e$  as compared to the **a1** model. The calcium charge decreased with the increasing number of surface-bonded water molecules.

**Dimethylphosphinic Acid and Dimethylphosphinothioic Acid Monoanions on the Hydroxyapatite Surface.** Dimethylphosphinic acid and dimethylphosphinothioic acid monoanion structures and their bidentate bonding to the calcium were optimized at the 3-21G(\*) basis set level in our earlier studies.<sup>2,3</sup> Those molecules were then bonded to the calcium of the HAP surface. The normal line to the  $xy$ -plane through the calcium was used again to define the direction in which the dimethylphosphinic acid monoanion approached the HAP surface. The molecule was a symmetric bidentate ligand in the bonding distance. The optimized and geometry-relaxed dimethylphosphinic acid monoanion maintained the bidentate bonding to the

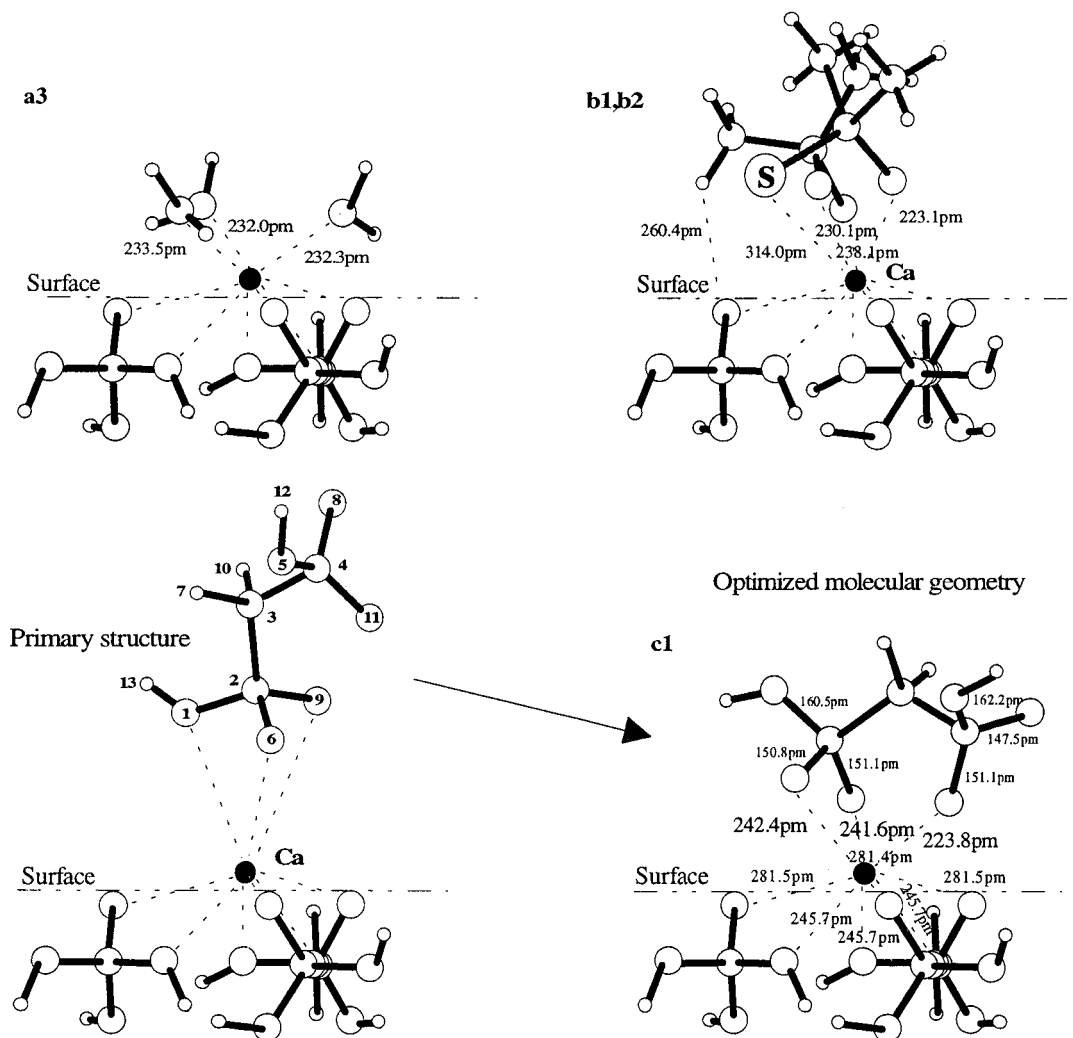


**Figure 1.** Calculated structures of the studied hydroxyapatite surface complexes. Three water molecules, two monoanionic dimethyl phosphinate species, and dianionic methylenebisphosphonate molecules are bonded to the surface calcium of HAP crystal.

**TABLE 1: Calculated  $\text{Ca}\cdots\text{O}$  Distances and Hydrogen Bond Lengths in HAP–Water Complexes **a1**, **a2**, and **a3** and HAP–Dimethylphosphinate **b1** and **b2** Complexes**

	length/pm			H-bond/pm		
	Ca–OH <sub>2</sub> <sup>1</sup>	Ca–OH <sub>2</sub> <sup>2</sup>	Ca–OH <sub>2</sub> <sup>3</sup>	H <sup>1</sup> –HAP	H <sup>2</sup> –HAP	H <sup>3</sup> –HAP
<b>a1</b>	227.1			195.4		
<b>a2</b>	228.9	230.4		188.7	205.1	
<b>a3</b>	232.0	232.3	233.5	183.9	190.2	192.6

	length/pm			H-bond/pm
	Ca–O <sup>1</sup>	Ca–O <sup>2</sup>	Ca–S <sup>2</sup>	H <sup>1</sup> –HAP
<b>b1</b>	238.1	230.1		260.4
<b>b2</b>	223.1		314.0	

surface calcium, but in the energetically preferred **b1** complex, the  $\text{Ca}\cdots\text{P}$  direction was deflected  $26^\circ$  from the normal line of the  $xy$ -plane through the calcium (Figure 1). The hydrogen bond-like interaction connected one hydrogen of the methyl group and one oxygen of the surface together. A distance of 260.4 pm for this weak  $\text{H}\cdots\text{O}$  interaction was calculated. Bonding distances between the surface calcium and the oxygens of the dimethylphosphinic acid anion were 230.1 and 238.1 pm. The symmetric bidentate bonding to the calcium is seen in Figure 1 and Table 1. The Mulliken charge of the calcium was  $0.49e$  in the **b1** model. As a comparison, the calcium charge was  $1.35e$  and the  $\text{Ca}\cdots\text{O}$  distances were 224 pm in the  $(\text{CH}_3)_2\text{PO}_2\text{-Ca}$  complex studied earlier.<sup>3</sup> The calcium charge decreased and the  $\text{Ca}\cdots\text{O}$  distances increased in the **b1** in relation to the

results calculated earlier for the “pure” ion pair. X-ray studies have been made for  $\text{Na}_2\text{HPO}_4$  species and  $\text{Na}\cdots\text{O}$  distances from 229 to 249 pm evaluated.<sup>59</sup>

The C–P–C angle was  $106.9^\circ$  in the  $(\text{CH}_3)_2\text{PO}_2\text{-Ca}$  complex,<sup>3</sup> and an almost similar value of  $105.8^\circ$  was determined for the **b1** complex. The P–O bond lengths in the **b1** were 152.3 and 15.8 pm. Those bond lengths shortened somewhat in relation to the P–O bonds calculated for the  $(\text{CH}_3)_2\text{PO}_2\text{-Ca}$  complex.<sup>3</sup> As a comparison, dimethyl phosphate species have been studied with different basis sets.<sup>60</sup> At the 3-21G(\*) basis set level values of 147.3 and 163.4 pm for P–O and P–O(C) bonds have been determined. With the MP2/6-31G\* method, corresponding bond lengths of 150.0 and 167.9 pm have been calculated, respectively.<sup>60</sup> Experimentally, values ranging from 149.0 to 149.8 pm for the P–O bonds and 153.6 to 158.2 pm for the P–O(C) bonds in dimethyl ammonium phosphate species have been determined.<sup>46</sup> X-ray studies have been made for anhydrous  $\text{Na}_2\text{HPO}_4$  crystal and P–O bond lengths from 151 to 156 pm and the P–O(H) bonds of 162 pm evaluated.<sup>59</sup>

The HAP crystal with dimethylphosphinothioic acid monoanions was studied using the method employed in the study of the **b1** complex. The sulfur–phosphorus compound as a bidentate ligand approached the surface from the direction guided by the normal line to the  $xy$ -plane through the calcium. The optimized complex structure **b2** was obtained. The bidentate metal bonding remained unchanged in the **b2** complex (Figure 1). The same bonding type was also found in the **b1**

TABLE 2: Calculated P–O, P–O(H), and P–C Bond Lengths and P–C–P Angles for Methylenebisphosphonate Molecules

		bond length/pm							angle/deg P–C–P	
		(H)O <sup>1</sup> –P <sup>2</sup>	(H)O <sup>5</sup> –P <sup>4</sup>	O <sup>6</sup> –P <sup>2</sup>	O <sup>8</sup> –P <sup>4</sup>	O <sup>9</sup> –P <sup>2</sup>	O <sup>11</sup> –P <sup>4</sup>	P <sup>2</sup> –C <sup>3</sup>		P <sup>4</sup> –C <sup>3</sup>
<b>c1</b>		160.5	162.2	150.8	147.5	151.1	151.1	178.9	183.8	114.28
<b>d1</b>	d1'	161.4	160.2	150.3	151.6	151.0	147.2	179.1	184.6	108.77
	d1''	161.4	160.2	150.3	151.6	151.1	147.2	179.1	184.6	108.75
<b>d2</b>	d2'	161.5	160.4	151.6	147.1	149.8	151.5	178.9	184.7	108.48
	d2''	161.5	160.4	151.6	147.1	149.8	151.5	178.9	184.7	108.48
<b>d3</b>	d3'	161.8	169.8	147.8	148.1	148.0	151.3	186.2	178.5	113.90
	d3''	160.1	160.4	146.8	151.7	152.2	150.6	184.8	178.8	109.49
	av		161.6				149.9		181.8	

TABLE 3: Calculated Ca···O Distances in the Methylenebisphosphonate Complexes and Relative Ca···O Distances in the Original HAP Crystal<sup>a</sup>

		length/pm					
		Ca–O <sup>1</sup>	Ca–O <sup>5</sup>	Ca–O <sup>6</sup>	Ca–O <sup>8</sup>	Ca–O <sup>9</sup>	Ca–O <sup>11</sup>
<b>c1</b>				242.4		241.6	223.8
<b>d1</b>	d1'			241.1	226.9	273.6	
	d1''			241.2	227.0	273.2	
<b>d2</b>	d2'			256.8		249.1	228.2
	d2''			256.7		249.2	228.4
<b>d3</b>	d3'		238.7				228.1
	d3''			256.4	223.6	238.8	

	length/pm								
	Ca–O <sup>A</sup>	Ca–O <sup>A</sup>	Ca–O <sup>A</sup>	Ca–O <sup>B</sup>	Ca–O <sup>B</sup>	Ca–O <sup>B</sup>	Ca–O <sup>C</sup>	Ca–O <sup>C</sup>	Ca–O <sup>C</sup>
HAP	245.7	245.7	245.7	281.5	281.4	281.5	240.7	240.7	240.8

<sup>a</sup> HAP crystal parameters Ca–O<sup>A,B,C</sup> from the work of Sanger and Kuhs.<sup>29</sup>

complex. The Ca···P direction was deflected 12° from the normal line of the *xy*-plane through the calcium. The optimized Ca···O and Ca···S interaction distances in the **b2** were 223.1 and 314.0 pm (Table 1). Ca···O and Ca···S bonds of 219 and 283 pm, respectively, were calculated earlier for the (CH<sub>3</sub>)<sub>2</sub>P(O)S·Ca ion pair.<sup>3</sup>

The Mulliken charge of the calcium in **b2** was 0.61*e*, and in the (CH<sub>3</sub>)<sub>2</sub>P(O)S·Ca species<sup>3</sup> the charge was 1.35*e*. The closest contact between the surface oxygens and the hydrogens of the methyl group in **b2** was 382.5 pm. A similar hydrogen bond effect as in **b1** was not found in **b2**. The C–P–C angle of 106.3° and P–O bond lengths from 154.2 to 154.6 pm and a P–S bond length of 203.0 pm were calculated for the (CH<sub>3</sub>)<sub>2</sub>P(O)S·Ca complex.<sup>3</sup> In **b2**, the corresponding C–P–C angle was 104.3° and the P–O and P–S bond lengths were 153.6 and 198.8 pm, respectively. The P–O and P–S bond lengths in the HAP-bonded species decreased slightly as compared to the corresponding values of the (CH<sub>3</sub>)<sub>2</sub>P(O)S·Ca pairs.

**Methylenebisphosphonic Acid Dianion on the Hydroxyapatite Surface.** Bonding to the HAP surface was also studied with methylenebisphosphonic acid dianion (H<sub>2</sub>MBP or methylenebisphosphonate). We have studied methylenebisphosphonate–calcium ion pairs theoretically in the previous paper in this series.<sup>5</sup> There, the calcium was found to bridge the three oxygen atoms of the monophosphonic acid ends of the molecule.<sup>5</sup> The interaction study of the methylenebisphosphonate–HAP system started from the primary structure, where one monophosphonic acid end of the bisphosphonate was bonded as a bidentate ligand to the surface calcium (Figure 1). The molecular geometry of the primary bisphosphonate structure was relaxed, and at the same time the bonding type to the calcium was changed. In the optimized structure **c1**, the original bidentate interaction was changed to the bridging type, where the entire methylenebisphosphonate molecule acted as a tridentate ligand for the metal bonding (Figure 1, Tables 2 and 3). In the optimized structure **c1**, the Ca···C line deflects 13° from the direction of the normal line to the *xy*-plane through the calcium. The tridentate bonding correlates well with our results

for the bisphosphonate–calcium and the bisphosphonate–calcium–water complexes,<sup>5</sup> where the bidentate calcium bonding to the monophosphonic acid end was found to be energetically unfavorable in relation to bridging the calcium site between the phosphorus groups.

The results obtained for **c1** suggested that on the HAP surface the oxygens of the monophosphonic acid ends were simultaneously bonded to the same calcium and that tridentate bonding had occurred (Figure 1). Tridentate calcium bonding is higher in energy than the energetically preferred tridentate type,<sup>5</sup> although the energy difference is somewhat smaller. The bisphosphonate studies with two calcium ions<sup>5</sup> suggested that in addition to the primary calcium bonding, as in the **c1** complex, secondary calcium bonding is also possible, where the monophosphonic acid ends act as bidentate ligands with other calciums on the three-dimensional bone surface.

In **c1**, the (H)O–P–C angles ranged from 100.8° to 103.6° and the O–P–C angles from 108.1° to 112.0°. The calcium was bonded simultaneously to the three oxygen atoms of this bisphosphonate. The distances from the surface calcium to the oxygens of the bisphosphonate were 223.8, 241.6, and 242.4 pm (Figure 1) (Table 3). In the bisphosphonate–calcium pair, these Ca···O distances were 213.9, 231.0, and 231.4 pm.<sup>5</sup> The bond lengths in the bisphosphonate–calcium pair were shorter than the bonds in the HAP–bisphosphonate complex. Increasing Ca···O distances in the HAP model in relation to the ion pairs were also found when dimethylphosphinic acid and dimethylphosphinothioic acid monoanions were bonded to the HAP surface instead of the free calcium. The steric hindrance around the calcium of the HAP model made the Ca···O distances longer than the Ca···O distances in the phosphinate–calcium and the bisphosphonate–calcium complexes, where compact ionic calcium can make close contacts with ligands.

The calculated Ca···O distances correlated well with the experimentally evaluated Ca···O distances of 236.2 pm reported for the CaCl<sub>2</sub>H<sub>2</sub>MBP·5H<sub>2</sub>O crystals.<sup>61</sup> The average, crystallographically determined Ca···O distances ranged from 239.2 to 257.0 pm for the four independent calcium coordinations in the

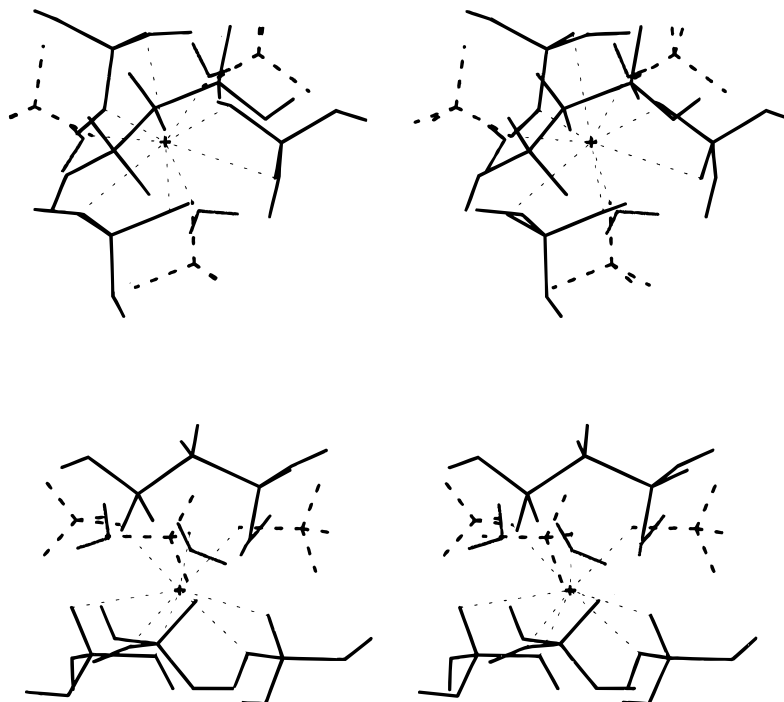


**Figure 2.** Hydroxyapatite crystal model (calcium and six neighboring phosphorus groups) as a stereo pair. Dotted hair line show original Ca coordination in the HAP crystal, and heavy dotted lines are used to present phosphorus groups removed. Calculated coordination models of HAP crystal surface with three water molecules and methylenebisphosphonate are fitted on the original HAP model.

$\beta$ -calcium diphosphate species.<sup>24</sup> In the methylenebisphosphonate–HAP model **c1**, the average P–O(H) and P–O bond lengths were 161.4 and 150.1 pm. The P–O(H) and P–O bonds correlated well with the corresponding average values of 158.1 and 150.9 pm calculated for the different bisphosphonate–calcium complexes.<sup>5</sup> As a comparison, the P–O(H) and P–O bonds in the crystal structure of  $\text{CaCl}_2\text{H}_2\text{MBP}\cdot 5\text{H}_2\text{O}$  were 155.8 and 149.6 pm, respectively.<sup>61</sup> The P–O bonds were 149.7 and 152.9 pm in the crystal structure of  $\beta$ -calcium diphosphate.<sup>24</sup> A P=O bond length of 145.5 pm for vinylphosphoryl dichloride species has been experimentally evaluated.<sup>19</sup> Theoretically, the P=O bond lengths calculated with the MP2/6-31G\* method for vinylphosphonic acid, vinylphosphoryl dichloride, and vinylphosphine oxide were 148.9, 148.4, and 150.1 pm, respectively.<sup>19</sup> The HF/6-311++G\*\* studies for the orthophosphate species have predicted P=O and P–O bond lengths of 144.6 and 157.1 pm, respectively,<sup>21</sup> and similar P=O and P–O bond lengths have been calculated by different basis sets for the pyrophosphate species.<sup>21,22</sup> In the anhydrous disodium hydrogenphosphate crystal structure, the average P–O and P–O(H) bond lengths were 153 and 162 pm, respectively.<sup>59</sup> P–O–P angles have ranged from 112.5° to 148.0°, and the internal hydrogen bond bridges between the phosphorus ends of the pyrophosphate molecules have been determined for the energetically preferred conformations.<sup>21,22</sup>

The Mulliken charge of the calcium in the HAP crystal model was 0.30 $e$ , and in the corresponding bisphosphonate–calcium pair the calcium charge was 1.08 $e$ .<sup>5</sup> The phosphorus charges were 1.59 $e$  and 1.66 $e$  in the HAP-bonded methylenebisphosphonate, and phosphorus charges of 1.60 $e$  and 1.65 $e$  were calculated for the energetically preferred bisphosphonate–calcium complex.<sup>5</sup> In the model, where six water molecules were hydrogen-bonded to the bisphosphonate,<sup>4</sup> phosphorus charges of 1.52 $e$  and 1.55 $e$  were calculated. The charges of phosphorus atoms increased as the metal ion complex was formed. The calcium charge was 0.30 $e$  in **c1**. Energetically preferred bisphosphonate–calcium and bisphosphonate–calcium–

[water]<sub>6</sub> complexes have calcium charges of 1.08 $e$  and 0.47 $e$ , respectively.<sup>5</sup>

The P–C–P angle of the methylenebisphosphonate was 114.3° in **c1**, and the angle decreased 2° as compared to the value of the methylenebisphosphonate–calcium complex. In the crystal structure of  $\text{CaCl}_2\text{H}_2\text{MBP}\cdot 5\text{H}_2\text{O}$ , a P–C–P angle of 114.8° was determined,<sup>61</sup> and it compares well with the P–C–P angle of our study.

The atoms of the original HAP crystal and the calculated complex structures **a3** and **c1** were superimposed. The differences between the calcium coordinations in the original HAP model and the calculated **a3** and **c1** complexes were considered (Figure 2). The calcium-bonded oxygen atoms in the water and the bisphosphonate molecules were almost at the same distances as the oxygens of the original HAP crystal structure, as seen in Figure 2. The results suggest that, in the other crystal directions, the oxygens of the calcium-bonded molecules are also coordinated in the same directions as the oxygens of the original HAP crystal.

**Calcium with Two Methylenebisphosphonic Acid Dianions.** Three different conformations of methylenebisphosphonate–calcium–methylenebisphosphonate complexes were considered. The P–C–P backbones of the bisphosphonates were parallel, perpendicular, and consecutive to either side of the calcium ion. The first two primary conformations included the bisphosphonates as tetradentate ligands bound to the calcium. In the third conformation, both bisphosphonates had monophosphonic acid ends, which acted as bidentate ligands to the calcium. All the primary molecular geometries and interaction distances in the bisphosphonate–calcium–bisphosphonate complexes were relaxed. Fully optimized, stable structures **d1**, **d2**, and **d3** were obtained. The three different conformations are seen in Figure 3.

In the energetically preferred conformation **d1**, the six-coordinated calcium ions were bridge-bonded between the ends of the methylenebisphosphonate molecules. The monophosphonic acid groups were rotated around the C–P axis during

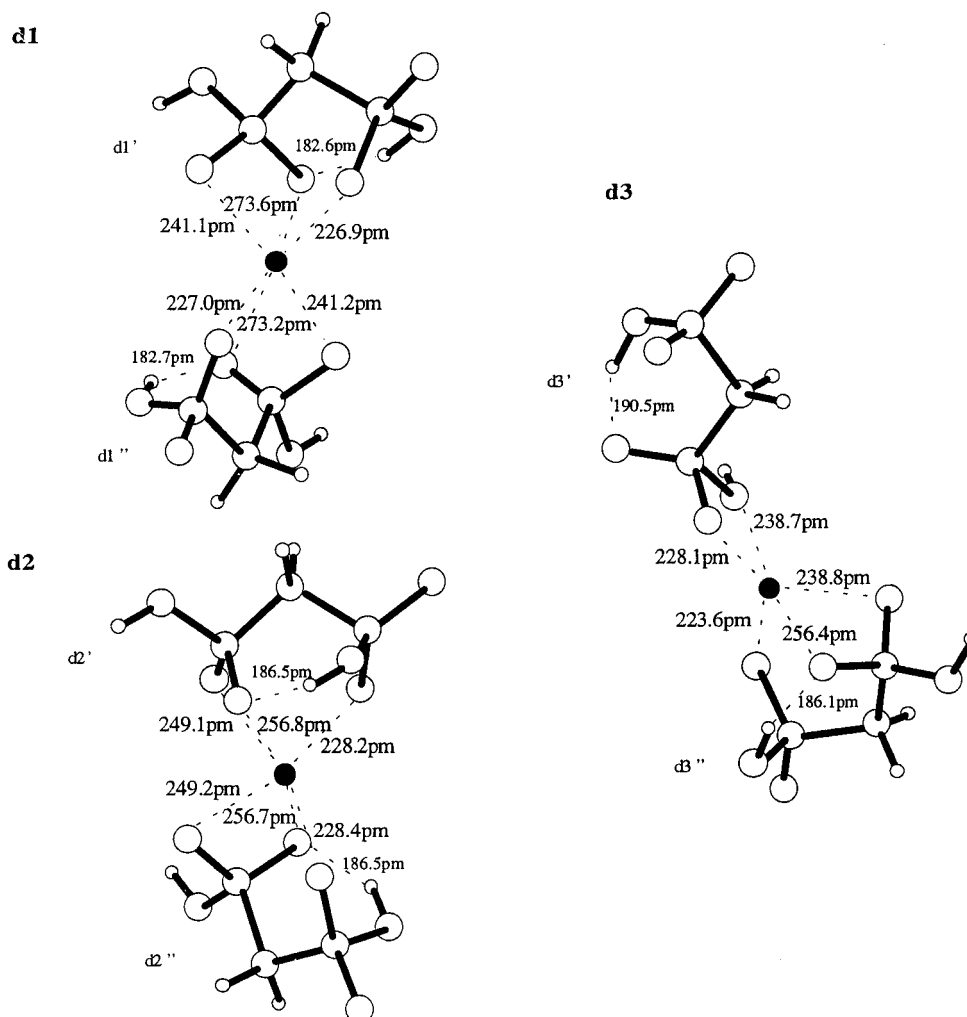


**Figure 3.** Three calculated conformations of the methylenebisphosphonate-calcium-methylenebisphosphonate complexes. The  $\text{Ca}\cdots\text{O}$  distances and the internal hydrogen bonds are presented.

the relaxation of the molecular backbones, and tridentate bonding was formed on either side of the calcium (Figure 3). The same geometrical changes in the molecular backbones were found in the bisphosphonate-metal complexes studied in a previous paper in this series.<sup>4</sup> Interaction distances between calcium and the nearest six oxygen atoms ranged from 226.9 to 273.6 pm, and the P-C-P angles of the bisphosphonates **d1'** and **d1''** were 108.8° and 108.7°, respectively (Figure 3, Tables 2 and 3). On either side of the calcium, the backbones of the bisphosphonate molecules were staggered relative to each other. The optimized six-coordinated calcium sphere in the **d1** complex was very compact, and there was no space left for other molecules to come into such close contact with the calcium as the two calcium-bonded bisphosphonate molecules. The average interatomic torsional angles of (H)O-P $\cdots$ P-O(H) backbones in the **d1'** and **d1''** molecules were 279°. Water molecules of the solvent sphere may form hydrogen-bonded bridges between the oxygen atoms of different bisphosphonate molecules in the aqueous solvents.

In the second conformation, **d2**, interaction distances  $\text{Ca}\cdots\text{O}$  ranged from 228.2 to 256.8 pm to the six neighboring oxygens (Figure 3, Table 3). The P-C-P angles in the complexes **d2'** and **d2''** bisphosphonates were 108.5° (Table 2). The angles were similar to those calculated for the global minimum energy conformation **d1**. On either side, the calcium-bonded bisphosphonate backbones were almost parallel with respect to each other. The average interatomic torsional angles of (H)O-P $\cdots$ P-O(H) in the bisphosphonate molecules were about 78°.

The coordination sphere of the calcium in **d2** was closed by the bisphosphonates, and no additional molecules could be bonded to the calcium. The coordination number of the calcium was the same as found in the **d1** complex.

In the third original conformation, the bisphosphonates were found on either side of the calcium ion as bidentate ligands. In the optimized complex geometry **d3**, there was only one original bidentate bisphosphonate ligand left. Another bisphosphonate was moved so that it acted as a tridentate ligand, where three oxygens of the molecule were bonded to the calcium. The coordination number of the calcium was five and the calcium ion was bonded to the oxygens in the range 228.1–256.4 pm (Table 3). The P-C-P angles were 113.9° in the bidentate molecule **d3'** and 109.5° in the tridentate **d3''** bisphosphonate (Figure 3, Table 2). The P-C-P angles were strongly affected by ionic interactions, but there were also internal hydrogen bonds between the monophasphonic acid ends of the bisphosphonates. The interatomic torsional angles of (H)O-P $\cdots$ P-O(H) in the bisphosphonate molecules were about 77° and 84°. In the different conformations, **d1**, **d2**, and **d3**, the effective internal hydrogen bonds ranged from 182.7 to 186.5 pm in the bisphosphonate molecules of **d1'**, **d1''**, **d2''**, and **d3'**, where tridentate bonding to the calcium was found. In the bidentate ligand molecule **d3''**, the hydrogen bond length was 190.5 pm. In the bisphosphonate-calcium-bisphosphonate complexes, the determined internal hydrogen bond lengths were comparable to the corresponding values for the bisphosphonate-water complexes and to the hydrogen bond lengths of the various

**TABLE 4: Calculated Total Energies at the 3-21G(\*) Level and the Results with MP2/3-21G(\*)/3-21G(\*) Method, Including the Total Solvation Energies ( $E_{\text{solv}}$ ) Calculated by Subtracting the SCF Energies from the SCRF Energies**

	3-21G(*) <i>E</i> /au	MP2 <i>E</i> /au	SCRF <i>E</i> /au	solvation $E_{\text{solv}}$ /kJ mol <sup>-1</sup>
HAP	-2589.532 479	-2591.125 235	-2589.824 716	-767.3
<b>a1</b>	-2665.097 693	-2666.839 522	-2665.357 701	-682.7
<b>a2</b>	-2740.762 418	-2742.632 194	-2741.003 359	-632.6
<b>a3</b>	-2816.420 542	-2818.418 606	-2816.648 214	-597.8
<b>b1</b>	-3156.684 291	-3158.833 367	-3156.813 639	-339.6
<b>b2</b>	-3477.870 188	-3480.026 509	-3478.005 455	-355.1
<b>c1</b>	-3755.072 194	-3757.700 528	-3755.186 503	-300.1
<b>d1</b>	-3004.063 789	-3005.956 550	-3004.323 738	-682.5
<b>d2</b>	-3004.060 232	-3005.954 009	-3004.317 820	-676.3
<b>d3</b>	-3004.005 274	-3005.896 135	-3004.254 534	-654.4

bisphosphonate–calcium ion pairs we have reported earlier.<sup>4,5</sup> The hydrogen bond lengths were also comparable to the values calculated earlier for the pyrophosphite species.<sup>21,22</sup> In the  $\text{H}_4\text{P}_2\text{O}_7$  compound, calculations with Hartree–Fock/6-311++G\*\* and DZP basis sets have predicted two internal hydrogen bonds with lengths of 239 and 233.0 pm, respectively.<sup>21,22</sup> For dianionic  $\text{H}_2\text{P}_2\text{O}_7^{2-}$  species two internal hydrogen bonds with lengths of 194.0 pm have been calculated.<sup>22</sup> For lithium, sodium, and potassium pyrophosphates and their anionic species internal hydrogen bonds from 184.7 to 210.5 pm have been determined.<sup>22</sup>

The calculated values of the P–C–P angles in the methylenebisphosphonate–calcium–methylenebisphosphonate complexes **d1**–**d3** were similar to the values reached for the calcium–bisphosphonate–calcium complexes and the bisphosphonate structures with internal hydrogen bonds connecting the phosphorus ends together. As a comparison, the P–C–P angles were closed in relation to the value of 114.8° in the crystal structure of  $\text{CaCl}_2\text{H}_2\text{MBP}\cdot 5\text{H}_2\text{O}$ .<sup>61</sup> The range from 113.9° to 117.2° includes the P–C–P angles of several bisphosphonate crystal species.<sup>61</sup> P–O–P angles from 117° to 170° in pyrophosphate species have been reported at different basis set levels, and the value of 118.4° has been calculated with HF/6-31G\* and 112.5° with HF/6-311++G\*\* basis sets, respectively.<sup>21</sup>

The **d2** and **d3** conformations were 9.3 and 153.6 kJ mol<sup>-1</sup> higher in energy than the global minimum energy structure **d1**. The complexation seems to prefer the structures of the bisphosphonate molecules, where calcium was bonded between the monophosphonic acid ends. The calcium-bonding trend is the same, which was determined earlier for the bisphosphonate–calcium complexes.<sup>5</sup> The Mulliken charges of the calcium ions in the energetically different conformations **d1**, **d2**, and **d3** were 0.51*e*, 0.47*e*, and 0.67*e*, respectively. The charge of the entire tridentate-bonded bisphosphonate was -1.13*e* in the **c1** complex. In the **d** group complexes, the tridentate-bonded bisphosphonates **d1'**, **d1''**, **d2'**, **d2''**, and **d3''**, were charged in the range -1.1*e* to -1.26*e*, and the bidentate-acting ligand **d3'** was charged with -1.48*e*. The charges for the entire methylenebisphosphonate molecules we calculated earlier were -1.08*e* in the methylenebisphosphonate–calcium complex and -1.11*e* in the methylenebisphosphonate–calcium–[water]<sub>6</sub> complex.<sup>5</sup>

In the bisphosphonate–calcium–bisphosphonate complexes at the 3-21G(\*) basis set level, the average calculated P–O, P–O(H), and P–C bonds were 149.9, 161.6, and 181.8 pm, respectively. As a comparison, in the  $\text{CaCl}_2\text{H}_2\text{MBP}\cdot 5\text{H}_2\text{O}$  crystal structure values of 149.6, 155.8, and 185.0 pm for the P–O, P–O(H), and P–C bond lengths have been determined, and average values of the P–O, P–O(H), and P–C bond lengths of 150.0, 155.2, and 181.8 pm have been evaluated for several anions of bisphosphonates and bisphosphonic acids.<sup>61</sup> Calculations for pyrophosphoric acid and pyrophosphate monoanion species with the DZP basis set have determined average lengths of 145.1 and 146.2 pm for the P–O bonds and values of 155.3 and 158.2 pm for the P–O(H) bonds, respectively.<sup>22</sup> The  $\text{HPO}^-(\text{OH})_3$  (oxyphosphorane) monoanionic species have been calculated with RHF/6-31+G(d), MP2/6-31+G(d), and SCRF/6-31+G(d) methods, and values of 149.8, 153.1, and 150.4 pm for the P–O bond lengths and 164.7, 168.2, and 164.9 pm for the P–O(H) bonds, respectively, have also been calculated.<sup>26</sup>

**Model Reactions.** SCF and SCRF energies calculated at the 3-21G(\*) basis set level were used for the determination of the model reactions to predict the formation processes of the complexes. Correlation corrections were calculated with the MP2/3-21G(\*)/3-21G(\*) method. The energies for the model reactions were also studied with the energies determined by the MP2/3-21G(\*)/3-21G(\*) method (Table 4). The basis set superposition error (BSSE) was calculated for molecule pairs. The basis set superposition error for the  $\text{H}_2\text{PO}_4^- \cdot \text{Na}^+$  complex was 18% calculated at the 3-21G basis set level; when  $\text{Li}^+$  and  $\text{Mg}^{2+}$  were complexed to the same ion, the BSSE was below 5%.<sup>62</sup> The BSSE corrections of energies at the minimum basis set level ranged from 15% to 28% when malonate and formate ligands were complexed with the  $\text{Ca}^{2+}$  ion.<sup>63</sup> Better results for energies have been obtained with split valence basis sets.<sup>64</sup> At the 3-21G(\*) basis set level, we calculated BSSE corrections ranging from 3% to 9% for the various calcium complexes with phosphonate, phosphinate, and bisphosphonate species.<sup>3,5</sup> The counterpoise (CP) method that has been used is one of the most common calculation procedure for handling the BSSE correction.<sup>65</sup> BSSE corrections were omitted in our studies with the HAP surface if there were multimolecular systems with three or more compounds. This omission occurred because the BSSE of multimolecular aggregates was previously calculated only for small-size complexes, e.g. dimers to pentamers of hydrofluoride with methods up to MP2/6-31G(d,p).<sup>65</sup> The BSSE correction in our study was calculated at the 3-21G(\*) basis set level for interactions of two species (Table 5). The HAP model

**Model Reactions.** SCF and SCRF energies calculated at the 3-21G(\*) basis set level were used for the determination of the model reactions to predict the formation processes of the complexes. Correlation corrections were calculated with the MP2/3-21G(\*)/3-21G(\*) method. The energies for the model reactions were also studied with the energies determined by the MP2/3-21G(\*)/3-21G(\*) method (Table 4). The basis set superposition error (BSSE) was calculated for molecule pairs. The basis set superposition error for the  $\text{H}_2\text{PO}_4^- \cdot \text{Na}^+$  complex was 18% calculated at the 3-21G basis set level; when  $\text{Li}^+$  and  $\text{Mg}^{2+}$  were complexed to the same ion, the BSSE was below 5%.<sup>62</sup> The BSSE corrections of energies at the minimum basis set level ranged from 15% to 28% when malonate and formate ligands were complexed with the  $\text{Ca}^{2+}$  ion.<sup>63</sup> Better results for energies have been obtained with split valence basis sets.<sup>64</sup> At the 3-21G(\*) basis set level, we calculated BSSE corrections ranging from 3% to 9% for the various calcium complexes with phosphonate, phosphinate, and bisphosphonate species.<sup>3,5</sup> The counterpoise (CP) method that has been used is one of the most common calculation procedure for handling the BSSE correction.<sup>65</sup> BSSE corrections were omitted in our studies with the HAP surface if there were multimolecular systems with three or more compounds. This omission occurred because the BSSE of multimolecular aggregates was previously calculated only for small-size complexes, e.g. dimers to pentamers of hydrofluoride with methods up to MP2/6-31G(d,p).<sup>65</sup> The BSSE correction in our study was calculated at the 3-21G(\*) basis set level for interactions of two species (Table 5). The HAP model

**TABLE 5: Model Reactions for the Formation of Studied Model Systems**

reactants	products	<i>E</i> /kJ mol <sup>-1</sup>			
		3-21G(*)	MP2	SCRF	BSSE
1 HAP + H <sub>2</sub> O → HAP·(H <sub>2</sub> O) ( <b>a1</b> )	-245.3	-261.3	-192.7	65.5	
2 HAP + (H <sub>2</sub> O) <sub>2</sub> → HAP·(H <sub>2</sub> O) <sub>2</sub> ( <b>a2</b> )	-406.1	-433.9	-290.9		
3 HAP + (H <sub>2</sub> O) <sub>3</sub> → HAP·(H <sub>2</sub> O) <sub>3</sub> ( <b>a3</b> )	-493.3	-519.0	-349.7		
4 HAP + (CH <sub>3</sub> ) <sub>2</sub> P(O) <sub>2</sub> → HAP·(CH <sub>3</sub> ) <sub>2</sub> P(O) <sub>2</sub> ( <b>b1</b> )	-992.9	-1023.0	-378.1	141.0	
5 HAP + (CH <sub>3</sub> ) <sub>2</sub> P(O)S → HAP·(CH <sub>3</sub> ) <sub>2</sub> P(O)S ( <b>b2</b> )	-886.8	-919.0	-300.0	99.3	
6 HAP + MBP → HAP·MBP ( <b>c1</b> )	-1499.0	-1558.6	-405.9	213.4	
7 CaMBP + MBP → Ca(MBP) <sub>2</sub> ( <b>d1</b> )	-678.0	-584.9	-424.7	177.3	
8 HAP·(H <sub>2</sub> O) + MBP → HAP·MBP ( <b>c1</b> ) + H <sub>2</sub> O	-1253.8	-1297.3	-213.3	147.9	
9 HAP·(H <sub>2</sub> O) <sub>2</sub> + MBP → HAP·MBP ( <b>c1</b> ) + (H <sub>2</sub> O) <sub>2</sub>	-1092.9	-1124.6	-115.1		
10 HAP·(H <sub>2</sub> O) <sub>3</sub> + MBP → HAP·MBP ( <b>c1</b> ) + (H <sub>2</sub> O) <sub>3</sub>	-1005.7	-1039.7	-56.2		

was taken as one compound in the BSSE calculations. This presumption for the BSSE calculation of HAP crystal was made because the same crystal model was always compared with all the other interacting species. The BSSE corrections calculated for the phosphorus species in the HAP surface were from 11% to 22%, and for the HAP–water complex, the BSSE was 27%. The calculated level of the BSSE correction correlates with those BSSE values calculated earlier for various species.<sup>3,5,62–65</sup>

The SCRF calculations were made without cavitation and dispersion corrections, because these effects were not expected to significantly change the molecular geometries of the stationary points in the free energy surface.<sup>66</sup> The SCRF model used in this study provided only a qualitative model for the solvent effects in the model reactions. The total solvation energies calculated as differences between SCRF and SCF/3-21G(\*) energies were high, because the crystal model was frozen in the original hydroxyapatite form (Table 4). The calculated SCRF energies for different species were used in the model reactions (Table 5). One to three water molecules were added to the HAP surface. An exothermic SCRF reaction energy of  $-193 \text{ kJ mol}^{-1}$  was calculated for the HAP–water complex and  $-350 \text{ kJ mol}^{-1}$  for the HAP–[water]<sub>3</sub> complex. When the hydroxyapatite–methylenebisphosphonate complex was formed from the corresponding reactants, an energy of  $-406 \text{ kJ mol}^{-1}$  was calculated by the SCRF method. Model reactions suggested that methylenebisphosphonate can replace HAP-bonded water molecules in the surface, and when HAP–[water]<sub>3</sub> was converted to the HAP–bisphosphonate, the SCRF reaction energy was  $-56 \text{ kJ mol}^{-1}$  (Table 5). If the BSSE corrections are estimated for all of the species of reactions (Table 5, reactions 2, 3, 9, 10), the resulting reaction energies converge to about  $-30 \text{ kJ mol}^{-1}$  in reactions 9 and 10. This result gives more support to the proposed complexation model, although the numerical value of the absolute reaction energy is very qualitative due to the large SCRF correction. In the complex **b2**, the effect of the sulfur atom decreased the formation energy below the energy of the three-water system **a3**. A destabilizing effect of sulfur was found in the phosphonate–calcium and phosphinate–calcium species,<sup>3</sup> and the same effect was also found in the HAP system of **b2**. The formation of the **b1** complex released an energy of  $-378 \text{ kJ mol}^{-1}$ . Energies of 406 and  $-425 \text{ kJ mol}^{-1}$  were released when complexes **c1** and **d1** were formed.

## Conclusions

In this study, interactions between the dicationic calcium ion and various types of anionic phosphorus species were calculated by *ab initio* molecular orbital methods. The molecular structures were fully optimized. The results suggest that in the HAP complexes the phosphorus compounds were bonded to the surface calcium in a similar way as in the calcium-bonded molecules in the ion pairs and in the water sphere clusters.<sup>2–4</sup> The bonding of the molecules to the HAP surface was orientated as much as possible in a similar way to the calcium coordination in the original HAP crystal structure. Similarities in the coordination spheres were seen when the HAP–[water]<sub>3</sub> and HAP–bisphosphonate species were compared to the original HAP crystal structure. In particular, the oxygens of the three water molecules were very close to those oxygen atoms of the crystal model. Hydrogen bonds were formed to link water molecules to the HAP surface. The dimethylphosphinic acid and dimethylphosphinothioic acid monoanions acted as bidentate ligands with the HAP surface. In the case of methylenebisphosphonate bonding, the two oxygens of the bisphosphonate were almost similar to the oxygens of the original crystal structure.

Two methylenebisphosphonates can be bonded to the calcium at the same time, forming the bisphosphonate–calcium–bisphosphonate complexes. Bridging type bonding was preferred, and the six-coordinated calcium ions there were tridently bonded as links between the monophosphonic acid ends of the bisphosphonates. The complex structures were very compact. The other calcium-bonding sites in the bisphosphonate backbone were higher in energy than the preferred bridging type. The monophosphonic acid ends of the bisphosphonate molecules were connected by strong internal hydrogen bonds. The theoretically calculated molecular geometries of the phosphorus species interacting with the HAP surfaces correlated well with the reference values of the experimental and theoretical studies of organophosphorus compounds. The calculated model reactions suggested that the methylenebisphosphonates may replace the water molecules on the HAP surface. The modeled formation of the HAP–methylenebisphosphonate system is energetically preferred in relation to the other complexes studied. In addition to the primary calciums of the HAP surface, which were tridentately bonded to the bisphosphonate ligand, the secondary calciums of the HAP surface may be bonded bidentately to the monophosphonic acid ends of the bisphosphonate molecules.

## References and Notes

- (1) Peräkylä, M.; Pakkanen, T. A.; Björkroth, J.-P.; Pohjala, E. *J. Chem. Soc., Perkin Trans. 2* **1992**, 1167.
- (2) Räsänen, J. P.; Peräkylä, M.; Pohjala, E.; Pakkanen, T. A. *J. Chem. Soc., Perkin Trans. 2* **1994**, 1055.
- (3) Räsänen, J. P.; Pohjala, E.; Pakkanen, T. A. *J. Chem. Soc., Perkin Trans. 2* **1994**, 2485.
- (4) Räsänen, J. P.; Pohjala, E.; Pakkanen, T. A. *J. Chem. Soc., Perkin Trans. 2* **1995**, 39.
- (5) Räsänen, J. P.; Pohjala, E.; Nikander, H.; Pakkanen, T. A. *J. Phys. Chem.* **1996**, *100*, 8230.
- (6) Van Rooijen, N. *Calcif. Tissue Int.* **1993**, *52*, 407.
- (7) Fleich, H. *Drugs* **1991**, *42*, 919.
- (8) Fonong, T.; Burton, D. J.; Pietrzyk, D. J. *Anal. Chem.* **1983**, *55*, 1089.
- (9) Quitasol, J.; Krastins, L. *J. Chromatogr. A* **1994**, *671*, 273.
- (10) Bonjour, J. B.; Rizzoli, R.; Ammann, P.; Chevalley, T. *Ann. Endocrinol. (Paris)* **1993**, *54*, 399.
- (11) Flanagan, A. M.; Chambers, T. J. *Bone Mineral* **1989**, *6*, 33.
- (12) Hannuniemi, R.; Lauren, L.; Puolijoki, H. *Drugs Today (Barcelona)* **1991**, *27*, 375.
- (13) Kanis, J. A.; McCloskey, E. V. *Calcium Metabolism. Prog. Basic Clin. Pharmacol.* **1990**, *4*, 89.
- (14) Papapoulos, S. E.; Landman, J. O.; Bijvoet, O. L. M.; Löwik, C. W. G. M.; Valkeama, R.; Pauwels, E. K. J.; Vermeij, P. *Bone* **1992**, *13*, 41.
- (15) Le Bideau, J.; Jouanneaux, A.; Payen, C.; Bujoli, B. *J. Mater. Chem.* **1994**, *4*, 1319.
- (16) Poojary, D. M.; Vermeulen, L. A.; Vicenzi, E.; Clearfield, A.; Thompson, M. E. *Chem. Mater.* **1994**, *6*, 1845.
- (17) Dejaegere, A.; Liang, X.; Karplus, M. *J. Chem. Soc., Faraday Trans.* **1994**, *90*, 1763.
- (18) Nair, H. K.; Guneratne, R. D.; Modak, A. S.; Burton, D. J. *J. Org. Chem.* **1994**, *59*, 2393.
- (19) Hernandez-Laguna, A.; Sainz-Diaz, C. I.; Smeyers, Y. G.; De Paz, J. L. G.; Galvez-Ruano, E. *J. Phys. Chem.* **1994**, *98*, 1109.
- (20) Rönkkömäki, H.; Lajunen, L. H. *J. Acta Chem. Scand.* **1995**, *49*, 36.
- (21) Colvin, M. E.; Evleth, E.; Akacem, Y. *J. Am. Chem. Soc.* **1995**, *117*, 4357.
- (22) Ma, B.; Meredith, C.; Schaefer, H. F. *J. Phys. Chem.* **1994**, *98*, 8216.
- (23) Uchamaru, T.; Tanabe, K.; Nishikawa, S.; Taira, K. *J. Am. Chem. Soc.* **1991**, *113*, 4351.
- (24) Taylor, M. G.; Simkiss, K.; Leslie, M. *J. Chem. Soc., Faraday Trans.* **1994**, *90*, 641.
- (25) Apaya, R. P.; Lucchese, B.; Price, S. L.; Vinter, J. G. *J. Comput.-Aided Mol. Des.* **1995**, *9*, 33.
- (26) Wladkowski, B. D.; Krauss, M.; Stevens, W. J. *J. Phys. Chem.* **1995**, *99*, 4490.
- (27) Le Bideau, J.; Payen, C.; Palvadeau, P.; Bujoli, B. *Inorg. Chem.* **1994**, *33*, 4885.



- (28) O'Brien, J. T.; Zeppenfeld, A. C.; Richmond, G. L.; Page, C. J. *Langmuir* **1994**, *10*, 4657.
- (29) Sängler, A. T.; Kuhs, W. F. Z. *Kristallogr.* **1992**, *199*, 123.
- (30) Rothwell, W. P.; Waugh, J. S.; Yesinowski, J. P. *J. Am. Chem. Soc.* **1980**, *102*, 2637.
- (31) Wong, A. T.-C.; Czernuszka, J. T. *Colloids Surfaces A: Physicochem. Eng. Aspects* **1993**, *78*, 245.
- (32) El Feki, H.; Khattech, I.; Jemal, M.; Rey, C. *Thermochim. Acta* **1994**, *237*, 99.
- (33) Nordström, T.; Rotstein, O. D.; Romanek, R.; Asotra, S.; Heersche, J. N. M.; Manolson, M. F.; Brisseau, G. F.; Grinstein, S. *J. Biol. Chem.* **1995**, *270*, 2203.
- (34) Handschin, R. G.; Stern, W. B. *Calcif. Tissue Int.* **1992**, *51*, 111.
- (35) Fernandez, V. L.; Reimer, J. A.; Denn, M. M. *J. Am. Chem. Soc.* **1992**, *114*, 9634.
- (36) Hauschka, P. V.; Carr, S. A. *Biochemistry* **1982**, *21*, 2538.
- (37) Hauschka, P. V.; Wians, F. H., Jr. *Anatom. Rec.* **1989**, *224*, 180.
- (38) Wang, J.; Caffrey, M. *J. Am. Chem. Soc.* **1995**, *117*, 3304.
- (39) (a) Frisch, M. J.; Head-Gordon, M.; Trucks, G. W.; Foresman, J. B.; Schlegel, H. B.; Raghavachari, K.; Robb, M. A.; Binkley, J. S.; Gonzalez, C.; Defrees, D. J.; Fox, D. J.; Whiteside, R. A.; Seeger, R.; Melius, C. F.; Baker, J.; Martin, R. L.; Kahn, L. R.; Stewart, J. J. P.; Topiol, S.; Pople, J. A. *GAUSSIAN90*; Gaussian Inc.: Pittsburgh, PA, 1990. (b) Frisch, M. J.; Head-Gordon, M.; Trucks, G. W.; Gill, P. M. W.; Wong, M. W.; Foresman, J. B.; Johnson, B. G.; Schlegel, H. B.; Robb, M. A.; Replogle, E. S.; Gomperts, R.; Anders, J. L.; Raghavachari, K.; Binkley, J. S.; Gonzalez, C.; Martin, R. L.; Fox, D. J.; Defrees, D. J.; Baker, J.; Stewart, J. J. P.; Pople, J. A. *GAUSSIAN92*; Gaussian Inc.: Pittsburgh, PA, 1992.
- (40) Ma, B.; Xie, Y.; Shen, M.; von Rague Schleyer, P.; Schaefer, H. F., III. *J. Am. Chem. Soc.* **1993**, *115*, 11169.
- (41) Ma, B.; Xie, Y.; Shen, M.; Schaefer, H. F., III. *J. Am. Chem. Soc.* **1993**, *115*, 1943.
- (42) Wu, Y.-D.; Houk, K. N. *J. Am. Chem. Soc.* **1993**, *115*, 11997.
- (43) Dobbs, K. W.; Hehre, W. J. *J. Comput. Chem.* **1986**, *7*, 359.
- (44) Cramer, C. J.; Dykstra, C. E.; Denmark, S. E. *Chem. Phys. Lett.* **1987**, *136*, 17.
- (45) Kwiatkowski, J. S.; Leszczynski, J. *Mol. Phys.* **1992**, *76*, 475.
- (46) Liang, C.; Ewig, C. S.; Stouch, T. R.; Hagler, A. T. *J. Am. Chem. Soc.* **1993**, *115*, 1537.
- (47) Thatcher, G. R. J.; Campbell, A. S. *J. Org. Chem.* **1993**, *58*, 2272.
- (48) Colson, A.-O.; Besler, B.; Sevilla, M. D. *J. Phys. Chem.* **1993**, *97*, 8092.
- (49) Rivail, J. L.; Rinaldi, D. *Chem. Phys.* **1976**, *18*, 233.
- (50) Rivail, J. L.; Terryn, B. *J. Chim. Phys.* **1982**, *79*, 2.
- (51) Rinaldi, D. *Comput. Chem.* **1982**, *6*, 155.
- (52) Rinaldi, D.; Ruiz-Lopez, M. F.; Rivail, J. L. *J. Chem. Phys.* **1983**, *78*, 834.
- (53) Atkins, P. W. *Physical Chemistry*; Oxford University Press: Oxford, 1990; p 952.
- (54) Rinaldi, D.; Pappalardo, R. R. *SCRFPAC: QCPE*, program No. 622; Indiana University: Bloomington, IN, 1992.
- (55) Tomasi, J.; Persico, M. *Chem. Rev.* **1994**, *94*, 2027.
- (56) *Sybyl*, Molecular Modeling Software, Version 6.03; Tripos Associates, Inc.: St. Louis, MO, 1993.
- (57) Åkesson, R.; Pettersson, L. G. M.; Sandström, M.; Siegbahn, P. E. M.; Wahlgren, U. *J. Phys. Chem.* **1992**, *96*, 10773.
- (58) Markham, G. D.; Bock, C. W. *J. Phys. Chem.* **1995**, *99*, 10118.
- (59) Baldus, M.; Meier, B. H.; Ernest, R. R.; Kentgens, A. P. M.; Meyer zu Altenschildesche, H.; Nesper, R. *J. Am. Chem. Soc.* **1995**, *117*, 5141.
- (60) Landin, J.; Pascher, I.; Cremer, D. *J. Phys. Chem.* **1995**, *99*, 4471.
- (61) Nardelli, M.; Pelizzi, G.; Staibano, G.; Zucchi, Z. *Inorg. Chim. Acta* **1983**, *80*, 259.
- (62) Alexander, R. S.; Kanyo, Z. F.; Chirlian, L. E.; Christianson, D. W. *J. Am. Chem. Soc.* **1990**, *111*, 249.
- (63) Maynard, A. T.; Hiskey, R. G.; Pedersen, L. G.; Koehler, K. A. *J. Mol. Struct. (THEOCHEM)* **1985**, *124*, 213.
- (64) Shiratori, Y.; Nakagawa, S. *J. Comput. Chem.* **1991**, *12*, 717.
- (65) Turi, L.; Dannenberg, J. J. *J. Phys. Chem.* **1993**, *97*, 2488.
- (66) Antonczak, S.; Ruiz-Lopez, M. F.; Rivail, J. L. *J. Am. Chem. Soc.* **1994**, *116*, 3912.